EQUILIBRIUM CONFIGURATIONS OF OXYGEN BUBBLES ON SURFACES FOR APPLICATIONS IN NANOSTRUCTURED HEMATITE ELECTRODES

By

Jennie Olivia Zheng

Submitted to the Department of Materials Science and Engineering in Partial Fulfilment of the Requirements for the Degree of

Bachelor of Science in Materials Science and Engineering

at the

Massachusetts Institute of Technology

June 2015

Signature redacted

Signature of Author .....
Jennie Olivia Zheng
Department of Materials Science and Engineering
May 1, 2015

Signature redacted

Certified by .....
W. Craig Carter
POSCO Professor of Materials Science and Engineering
Thesis Supervisor

Signature redacted

Accepted by .....
Geoffrey Beach
Associate Professor of Materials Science and Engineering
Undergraduate Committee Chairman

EQUILIBRIUM CONFIGURATIONS OF OXYGEN BUBBLES ON SURFACES FOR APPLICATIONS IN NANOSTRUCTURED HEMATITE ELECTRODES

By

Jennie Olivia Zheng

Submitted to the Department of Materials Science and Engineering

on May 8, 2015 in Partial Fulfilment of the

Requirements for the Degree of

Bachelor of Science in Materials Science and Engineering

ABSTRACT

The variability of a nanostructured material's fundamental properties as compared to its bulk state has led to the rich field of nanotechnology and the quest to uncover unique properties of structures at the nanoscale. An active application for these materials is in the nanostructuring of α-Fe_2O_3 (hematite) for photoelectrochemical (PEC) splitting of water to generate hydrogen. A model of a bubble on a nanorod was developed in this work to facilitate the understanding of equilibrium configurations of oxygen bubbles on a nanostructured hematite electrode. The equilibrium configurations are computed using Surface Evolver, a program which models surfaces shaped by various constraints and forces. A nanorod with a top surface dimension of 100 by 100 nm was the subject of the bulk of this work. The energy of different starting configurations of the bubble and increasing volume of the bubble were compared to that of a free spherical bubble. The energy of the bubble approaches the total surface energy of a free spherical bubble, indicating that a bubble that has nucleated on the surface of a nanorod will approach a shape that has nearly the same energy as a detached spherical bubble. For applications in PEC splitting of water, this result indicates that from an equilibrium and lowest energy perspective, an oxygen bubble could nucleate on the surface of a nanorod, grow in volume, and detach or pinch-off from the nanorod.

Thesis Supervisor: W. Craig Carter

Title: POSCO Professor of Materials Science and Engineering

Acknowledgements

I would first like to acknowledge the support and guidance of my thesis advisor, Professor W. Craig Carter. He has been my mentor throughout my entire time in the department, from a curious sophomore to a senior who will be continuing further with graduate studies. He has supervised my growth as a student and as a confident researcher—for that I will be eternally grateful. Even when he was extremely busy with his own work, he still found time to entertain my questions and help me through my struggles with this research. I love his enthusiasm and energy when it comes to education and to fundamental materials science research, which he is able to blend together in beautiful concert through classes I have had the privilege to take. Throughout the years, I have been able work with Professor Carter as a TA for 3.016 which has been a fantastic teaching experience. Through his numerous international collaborators, I was able to work on a research collaboration with MISTI-Germany partners (Christina Scheu and Alexander Müller) and Rachel Zucker. I thank them for their support and collaborative efforts with this work.

I would also like to thank two other professors that have made an immense impact on my life and research trajectory: Professor Jeffrey Grossman and Professor Niels Holten-Andersen. Professor Jeffrey Grossman for giving me the opportunity to join his research group as a freshman. I learned so much during those formidable years about being a researcher and always striving to tackle the toughest challenges. Without his terrific mentorship throughout the years, I would not have been exposed to all the opportunities within Course 3. His passion and enthusiasm for materials science and teaching is infectious and something I always strive for myself. My departmental advisor, Prof. Niels Holten-Andersen has always offered so much support for any undertaking or endeavor that I chose to pursue. He was there to guide me through my first completely independent research project, from which I learned so much.

Lastly, I would like to extend my gratitude to all my friends, family, and everyone I've interacted with during these past four years. I would be the person I am today without the love and support of everyone in my life. I have been so inspired by my peers here at MIT to strive reach for the stars—I am so grateful for the opportunity to make the world a better place.

Table of Contents

Introduction

Although solar energy is the most abundant energy source, wide-scale adoption of solar energy technology hinges on improved means of energy storage and higher energy conversion efficiencies. Energy storage is essential to compensate for the intermittency of solar energy due to cloudy conditions and variation of solar power over a day-night cycle. A very promising avenue for storing solar energy is through water-splitting systems, specifically photoelectrochemical (PEC) cells which convert sunlight directly into chemical energy by splitting water into oxygen and hydrogen (Fig. 1). PEC cells consists of a photoanode (typically a semiconductor) and a cathode (typically a metal) which undergo an oxygen evolution reaction and hydrogen evolution reaction, respectively. Large efficiency gains of photoelectrochemical cells can be improved through unique materials selection and design of the photoanode. Ideal materials to use as the photoanode of PEC cells would have a small bandgap for abundant solar absorption, high conversion efficiency of photogenerated carriers to the water splitting products, durability in aqueous environments, and—most importantly for wide-scale adoption—low cost.[1]

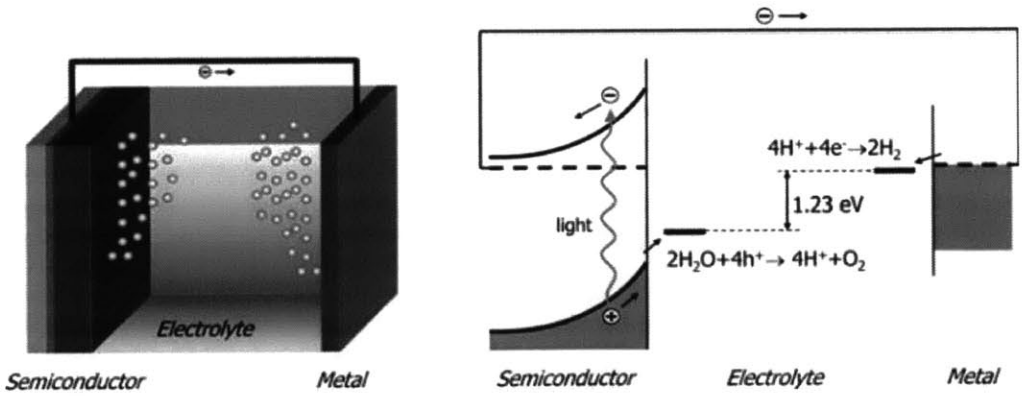

Figure 1. Schematic and band diagram of a photoelectrochemical cell showing the oxygen evolution reaction at the photoanode (represented here by a semiconductor) and the hydrogen evolution reaction at the cathode (represented here as a metal).[2]

Presently, no single material fulfils all these requirements so research has turned towards focusing on tandem cells such as a photoanode combined with a photovoltaic. A promising material for use as a photoanode is hematite (α-Fe_2O_3), a material that is abundant, low cost, and has the potential to convert 16.8% of the sun's energy into hydrogen[3]. The resulting hydrogen can then be used in fuel cells, the Haber-Bosch process, hydrocracking, and the production of synthetic fuels.

Due to fast electron-hole recombination rate of hematite photoanodes, surface modifications and structures on the nanoscale have been shown to increase the efficiency of hematite electrodes[1]—this has led attempts to nanostructure hematite electrodes. Currently, there is no comprehensive three-dimensional model of the oxygen bubble-electrodes interface that can account for the morphological and nanoscale-structuring effects on the efficiency of hematite photoanodes. Optimizing the nanostructure using computational methods give guidance in identifying morphologies that have the highest potential sunlight to hydrogen conversion efficiency. This efficiency is directly related to the active surface available to undergo the electrochemical reaction. An important factor in the optimization of the nanostructure of hematite photoanodes concerns the bubble formation on the surface of the electrode. Oxygen is released into the electrolyte by the hematite photoanode during the oxygen evolution reaction. As the electrolyte becomes saturated, oxygen bubbles eventually nucleate on the anode surface. Before the bubble detaches, the area of the bubble in contact with the anode becomes unable to catalyze further reaction because it is no longer in contact with the water. A model of the wetting behavior of the oxygen bubble on the surface electrode as a function of the nanostructure would allow tailoring of the hematite electrode for optimal PEC cell efficiency.

The bulk of this work uses the Surface Evolver software[4] (which models liquid surfaces shaped by various forces and constraints) to simulate bubble nucleation and detachment. Surface Evolver achieves this model by numerically computing the conditions of stability of a buoyant droplet or bubble attached to a variety of surfaces structure. The focus is looking at equilibrium shapes of bubbles in a nanostructured environment as a function of bubble volume and wetting behavior.

Theory

The Idea of an Interface

An interface is the geometrical surface that determines the boundary of two fluid domains.[5] While this mathematical definition implies that an interface has no thickness, the reality is more complex. The separation between the two fluids (water/oil, water/air, etc.) depends on the molecular interactions between the molecules of each fluid and on thermal agitation (Brownian diffusion). The microscopic interface between two fluids looks like the scheme shown in Fig. 2. However, in engineering applications, it is the macroscopic behavior of the interface that finds utility.

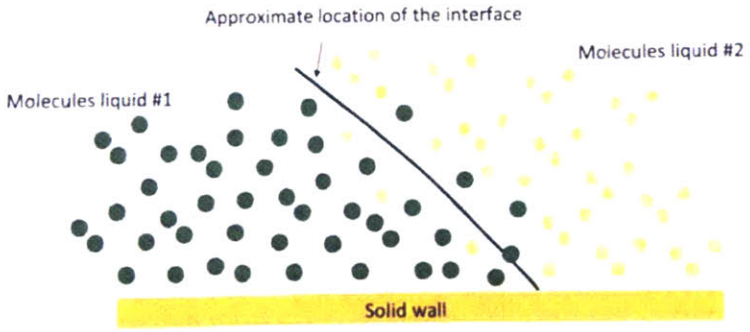

Figure 2. Schematic view of an interface at the molecular level[5]

From a macroscopic perspective, Fig. 2 can be replaced by the following figure (Fig. 3) which shows the interface as a mathematical surface without thickness and the contact angle θ is uniquely defined by the tangent to the surface at the contact line.[5]

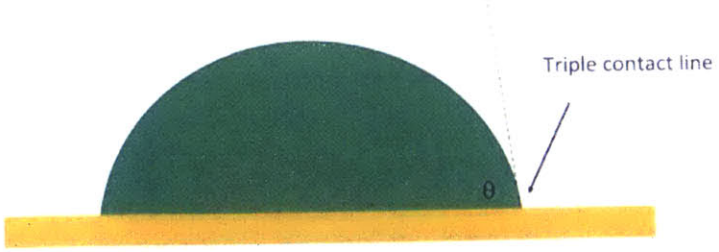

Figure 3. Macroscopic view of an interface of a drop on a substrate.[5]

Molecules attract each other in a condensed state. Molecules located in the bulk of a liquid have interactions (mostly van der Waals for organic liquids and hydrogen bonds for polar liquids) with similar molecules. In contrast, molecules at an interface interact with similar bulk molecules as well as molecules of the neighboring fluid.

At the interface between a fluid and a gas, the molecules in the liquid are less attracted to the gas side than the liquid side due to the low density and fewer interactions of the gas side. The local asymmetry in the interactions results in an excess of surface energy and a quantity called "surface tension" which takes into account this molecular effect. The dimensions of surface tension are energy per unit area or equivalently force per unit length.

A fluid system will always act to minimize surface area because the larger the surface area, the larger the number of molecules at the interfaces and the larger the cohesive energy imbalance. Molecules at the interface look for other molecules to equilibrate their interactions.

Surface tension is denoted by the Greek letter γ. For a homogeneous interface, the total energy of the surface is

$$E = \gamma S \tag{1}$$

where S is the interfacial surface area.

Surface tension increases as molecular size decreases and the intermolecular attraction increases.

liquid	γ_0	α
Acetone	25.2	−0.112
Benzene	28.9	−0.129
Benzylbenzoate	45.95	−0.107
Bromoform	41.5	−0.131
Chloroform	27.5	−0.1295
Cyclohexane	24.95	−0.121
Cyclohexanol	34.4	−0.097
Decalin	31.5	−0.103
Dichloroethane	33.3	−0.143
Dichloromethane	26.5	−0.128
Ethanol	22.1	−0.0832
Ethylbenzene	29.2	−0.109
Ethylene-Glycol	47.7	−0.089
Isopropanol	23.0	−0.079
Iodobenzene	39.7	−0.112
Glycerol	64.0	−0.060
Mercury	425.4	−0.205
Methanol	22.7	−0.077
Nitrobenzene	43.9	−0.118
Perfluorooctane	14.0	−0.090
Polyethylen-glycol	43.5	−0.117
PDMS	19.0	−0.036
Pyrrol	36.0	−0.110
Toluene	28.4	−0.119
Water	72.8	−0.1514

Table 1. Values of surface tension of different liquids in contact wth air at a temperature of 20°C (middle column, mN/m) and thermal coefficient α (right column, mN/m/°C).[5]

Derivation of the Young-Laplace Equation[5]

Suppose a fluid surrounds a spherical droplet of liquid. The work necessary to increase its volume from the radius R to the radius $R + dR$ (Fig. 4) arises from the internal volume increase,

pulling out the external fluid, and increasing the interfacial area. The work due to the internal volume increase is

$$\delta W_i = -P_0 dV_0 \tag{2}$$

Where dV_0 is the increase of the volume of the droplet,

$$dV_0 = 4\pi R^2 dR \tag{3}$$

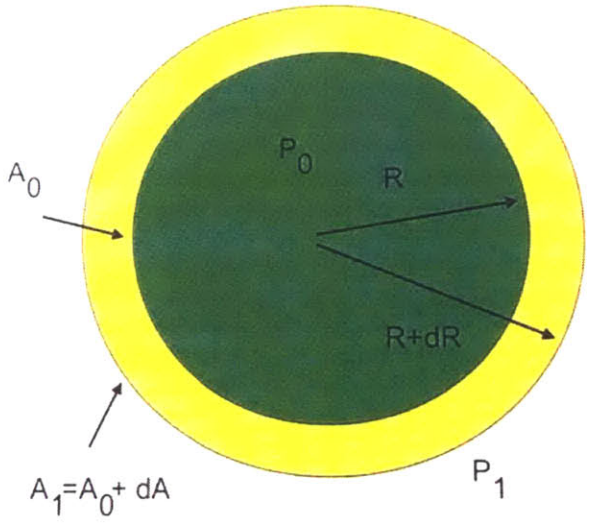

Figure 4. Schematic of a liquid droplet immersed in a fluid. Initially, the droplet has a radius of R and a surface area of A_0. An increase of its radius by dR corresponds to the new surface area A_1 and pressure P_1.[5]

The work to pull out the external fluid is

$$\delta W_e = -P_1 dV_1 \tag{4}$$

Where dV_1 is the decrease of the external volume, equal to $-dV_0$. The work corresponding to the increase of interfacial area is

$$\delta W_S = \gamma dA \tag{5}$$

Where dA is the increase of the surface area. The mechanical equilibrium condition is then

$$\delta W = \delta W_i + \delta W_e + \delta W_S = 0 \tag{6}$$

Using the values of work found previously and substituting, it follows that

$$\delta P = P_1 - P_0 = 2\frac{\gamma}{R} \tag{7}$$

Equation 7 is the Laplace equation for a sphere. The same reasoning can be applied to other geometries to achieve the generalized Laplace equation:

$$\delta P = \gamma \frac{dA}{dV} \tag{8}$$

For an interface locally defined by two (principal) radii of curvature R_1 and R_2, the result is

$$\delta P = \gamma(\frac{1}{R_1} + \frac{1}{R_2}) \tag{9}$$

The Young-Laplace equation expresses the local mechanical equilibrium between the liquid-vapor interface and its adjacent bulk phases and can also be given by

$$\Delta P = 2H\gamma \tag{10}$$

where ΔP is the pressure difference across the vapor-liquid interface, H is the mean curvature and γ is the interfacial tension. The Laplace pressure may be neglected for length scales smaller than the capillary length.[6] Capillary length is a characteristic length for an interface between a fluid and vapor which is subject to a surface force due to surface tension at the interface and gravity. It is defined as[7]

$$\lambda_c = \sqrt{\frac{\gamma}{|\Delta\rho|g}} \tag{11}$$

where γ is the surface tension of the vapor-fluid interface, $\Delta\rho$ is the difference in density of the fluids and g is the gravitational acceleration. If the droplet height exceeds a microscopic length λ_m that is approximately equal to 100 nm, contributions of the pressure difference become negligible.[8–10] In the

length scales between λ_c and λ_m, the free liquid interface of a static droplet is a surface of constant mean curvature.[11]

For calculation purposes, $\Delta\rho$ was taken to be 1000 kg/m^3, g was taken to be 9.8 N/kg and γ was 0.072 N/m (the surface tension between the air and water interface).

Pressure in a Bubble

The internal pressure in a bubble (assuming that the thickness of the liquid layer is negligible in front of the bubble radius R), is derived from the Young-Laplace equation (Fig. 5) to yield:

$$\delta P = 2\gamma\left(\frac{1}{R_{ext}} + \frac{1}{R_{int}}\right) = \frac{4\gamma}{R} \tag{12}$$

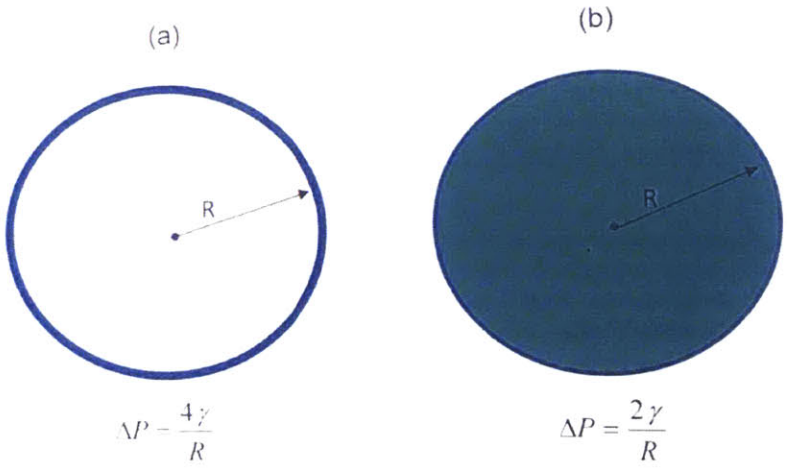

Figure 5. Internal pressure in a bubble (a) and in a droplet (b) of the same radius[5]

As long as the bubble size is micro- or milli- meter order, the Laplace equation can be used to explain the bubble dynamics.[12,13] The pressure difference between the liquid and vapor phase increases as in inverse power of R. For example, a bubble with R = 10 nm in water at room temperature ($\gamma = 0.072\ N/m$) will show an extraordinary pressure of about 150 atm.[14] Two

different theories attempt to explain the mechanical stability of this bubble under atmospheric pressure. One approach is to abandon the Young-Laplace equation and to assume it is only applicable in macroscopic or continuum level situations.[15] Another equation must replace the Young-Laplace equation that takes into account the atomic scale structure of the bubble surface. The second approach is to assume that the Young-Laplace equation still holds but that the surface tension differs from the macroscopic system.

Contact Angle Measurements

The shape of a gas bubble or liquid drop on a homogeneous, solid surface is dictated by the free energy of the three interfaces: solid/liquid, solid/vapor and liquid/vapor and by the topography of the surface.[16] The contact angle (angle between the tangent to the liquid surface and the tangent to the solid surface) is a characteristic parameter of the three-phase system and is used to describe the lyophilic/lyophobic properties of the solid surface and its quality.[17] Direct measurements of the contact angle from the profile of a sessile drop or an adhering gas bubble (Fig. 6)[16] is the most widely used experimental technique. In general, it is the most convenient method if a high degree of accuracy is not required. The advantages of this method are that very small quantities of liquid and substrate are necessary.

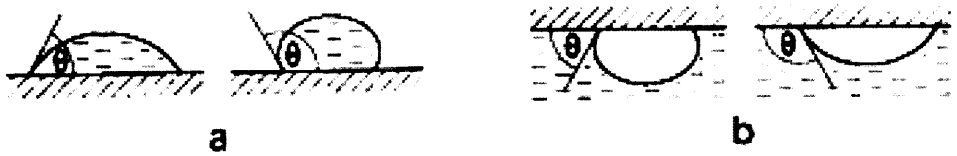

Figure 6. Schematic examples of (a) sessile drops on a solid surface and (b) adhering gas bubbles in a liquid underneath a solid surface with a nonzero contact angle.[5]

Surface Evolver Simulations

Computation of Droplet Shapes

The liquid-vapor interface of a liquid wetting a solid substrate on a sub-millimeter length scale to a few hundred nanometers is a surface of constant mean curvature in equilibrium.[11] For substrate geometries more complicated than a flat plane, the equilibrium shape is unknown, with the exception of a few high-symmetry cases. These substrates of high symmetry produce droplets shapes that can be explicitly parameterized.[6] Fortunately, approximations of the liquid shapes through simple surfaces of constant mean curvature can lead to asymptotically-exact results.[6] For other geometries, a discrete approximation to the surface can be found using computational methods. The liquid-vapor interface may be represented by a mesh of small triangles spanning neighboring nodes instead of using surfaces of constant mean curvature. The static droplet shapes that represent the local minima of the interfacial energy can be found through numerical minimization. During a minimization, the shape of the free liquid interface may undergo large changes, including mesh dilations and compressions.[6] The quality of the mesh is maintained through changes in the local topology through refinement techniques, including vertex averaging, equitriangulation, and deletion of tiny edges. Surface Evolver is one of many software programs that perform numerical minimizations using dynamically-triangulated surfaces.

Operating Surface Evolver

Surface Evolver is a program used to study surfaces shaped by various energies (including, but not limited to, surface tension and gravitational potential energy) and subject to constraints. The program minimizes the energy of the surface, which is approximated by vertices, edges and triangular facets. An initial surface is defined by vertices and edges which define the surfaces of triangular facets. These facets can be progressively refined during the evolution, which typically use the gradient and conjugate gradient descent methods.

Gradient and Conjugate Gradient Descent Method

The gradient descent method (*g* command) calculates the gradient of the energy function (a scalar function of all the vertex coordinates) and then moving each vertex in the direction of the negative gradient (line of motion) by some multiple of the gradient (given by the *scale*). Surface Evolver evaluates the energy for several scales along the line of motion to find the minimum energy. Successive steps in the gradient descent method are vectors orthogonal to each other.

The conjugate gradient method accelerates gradient descent by retaining a cumulative history vector and combining it with the gradient to determine the conjugate gradient direction. Convergence using the conjugate gradient method can occur faster when the evolution is close to the minimum in the energy landscape.

Best practice involves running the evolution with a few steps of ordinary gradient descent at the start or after major changes and using the conjugate gradient method for the bulk of the evolution.

Level Set Constraints

A constraint is a restriction of the motion of vertices and may be represented as a level set of a function or as a parametric manifold.[4] A level set constraint may have a vector field associated with it that is integrated over edges lying in the constraint to give an energy. This vector field is called the energy integrand and is useful for calculating gravitational energy and for specifying wall contact angle. Another possibility is that the level set constraint has a vector field associated with it that is integrated over edges lying in the constraint to give a volume contribution to a body whose boundary facets contain the edges (which is known as the content integrand). The content integrand is used to get the correct volume for bodies and is evaluated along the positive direction of the edge.

Energy

Surface Evolver minimizes the total energy of the surface, which can have several components including surface tension, gravitational potential energy, and constraint edge integrals.

Surface Tension

Interfaces between different fluids have an energy content proportional to their area; therefore, they shrink to minimize energy. This energy per unit area is also known as surface tension or force per unit length. In Surface Evolver, each facet has a surface tension which contributes to the total energy of the system.

Gravitational Potential Energy

A body contributes its gravitational energy to the total if the body has a density. The energy is defined as

$$E = \iiint_{body} GzdV \tag{13}$$

where G is gravity and V is volume.

Using the Divergence Theorem, Eq. 13 becomes

$$\iint_{surface} G\rho \frac{z^2}{2} \vec{k} \cdot \overrightarrow{dS} \tag{14}$$

where ρ is the density, $\frac{z^2}{2}$ is the function to be integrated over, $\vec{k}$ is a unit vector and $\overrightarrow{dS}$ is a surface vector.

This integral is done over each facet that comprises the body.

Constraint Edge Integrals

An edge on a constraint may have an energy given by integrating a vector field $\vec{F}$ over the oriented edge:

$$E = \int_{edge} \vec{F} \cdot \overrightarrow{dl} \tag{15}$$

Volume or Content[4]

Bodies in Surface Evolver may have a volume specified in the datafile which then becomes a volume constraint. The volume of a body can be written as

$$V = \iiint_{body} 1 \, dV \tag{16}$$

which can be rewritten as the following using the Divergence Theorem:

$$V = \int_{surface} z\vec{k} \cdot \overrightarrow{dS} \tag{17}$$

Commands

Operating Surface Evolver involves typing and commands and pressing enter. The Surface Evolver manual[4] includes a detailed list of commands and example files. The command "s" prompts a graphics window so the user can visualize the shape defined in the data-sheet.[18] A list of some of the possible commands can be viewed using the "h" command.

To evolve the surface, the gradient descent method ("g" command) is typically used. A number following each command indicates the number of steps of that particular command should be executed. For example, "g 5" executes 5 steps of the gradient descent method. The "r" command is used to refine the mesh. It can be applied to all facets or a particular set of facets that are defined to lie on a constraint. To prevent edges and vertices from running to each other, the user must refine the surface as it is evolving. Surface Evolver has a number of regrinding commands including ones to remove tine edges, equiangulate and vertex average. Useful single letter commands are included in Table 2.

Command	Description
h	Help screen
q	Exit
s	Screen display (native graphics)
g	Go one iteration step
r	Refine triangulation
u	Equiangulate
w	Weed out small triangles
V	Vertex averaging
v	Report volumes
b	Set body pressures
J	Toggle jiggling on every move

Table 2. Commonly used single letter commands in Surface Evolver.[4]

Datafile setup

The datafile for Surface Evolver is organized into six parts: Definitions and options, Vertices, Edges, Faces, Bodies and Initial commands.[4] The Definitions and options section begins the datafile and includes variables which must be specified before construction of the geometric elements. Relevant definitions for the purposes of this work include defining the gravity constant, buoyancy force and surface tension. Level set constraints are then declared to restrict the vertices and edges to lie on a particular line or surface and to properly define the energy and content integrals. After the level set constrains have been defined, the vertex list is constructed and is prefaced by VERTICES. The numbered vertices subsequently are used in the EDGES section to construct the edges of the shapes in the Surface Evolver simulation. The FACES section contains the numbered edges and are used to construct the faces of the shape in the Surface Evolver simulation. To finalize the construction of the structures within the Surface Evolver simulation, the BODIES section includes all the necessary bodies, volume and densities. The last section is the READ section which contains commands which are read and executed before commands are entered into the command prompt.

Results & Discussion

Bubble on Rod

The stability and liftoff volume of a bubble on a rod were simulated using Surface Evolver. Fig. 7 depicts a schematic of the initial configuration of the bubble on a rod.

Figure 7. Schematic of the initial bubble shape (blue) on a rod (orange).

The following computational calculations involving a bubble on a rod neglect the side lengths of the rod and focus solely on the top surface of the rod. Graphic files that were generated using Surface Evolver represent the surface of the bubble with a green mesh and the top surface of the rod with and orange mesh.

Estimation of Liftoff Volume

Relevant parameters in this system include volume, V [m^3], density, ρ [kg/m^3], surface tension, γ [J/m^2 or kg/s^2], gravity, g [m/s^2], and the characteristic length of the system, L [m^3]. Rearranging these parameters yields the relationship between the characteristic length scale and gravity, density, volume and surface tension.

$$L = \frac{g\Delta\rho V}{\gamma} \tag{18}$$

where $\Delta\rho$ is the difference in density between the bubble and the surrounding fluid.

For the bubble on a rod, the characteristic length scale of the system is the width of the rod. The buoyant force for the bubble is approximately equal to the surface tension times the characteristic length:

$$\Delta\rho g V \cong \gamma L \tag{19}$$

The volume at liftoff can be estimated by rearranging Eq. 19,

$$V \cong \frac{\gamma L}{\Delta\rho g} \tag{20}$$

One Unpinned Vertex

In this study, Surface Evolver is used to simulate a bubble on a rod with top surface shaped as a square (Appendix, Part A). One of the vertices of the initial bubble was unpinned from the corner of the rod surface. The edge lengths for the square (characteristic length) were varied from 1 mm to 8 mm. The contact angle of the bubble with the surface was 90°. The energy of the shape is plotted against the characteristic length of the rod in Fig. 8 and against the volume of the bubble in Fig. 9. The volume of the bubble and characteristic length of the system were coupled. Between a characteristic rod length of 4 and 6 mm, the energy reaches a maximum.

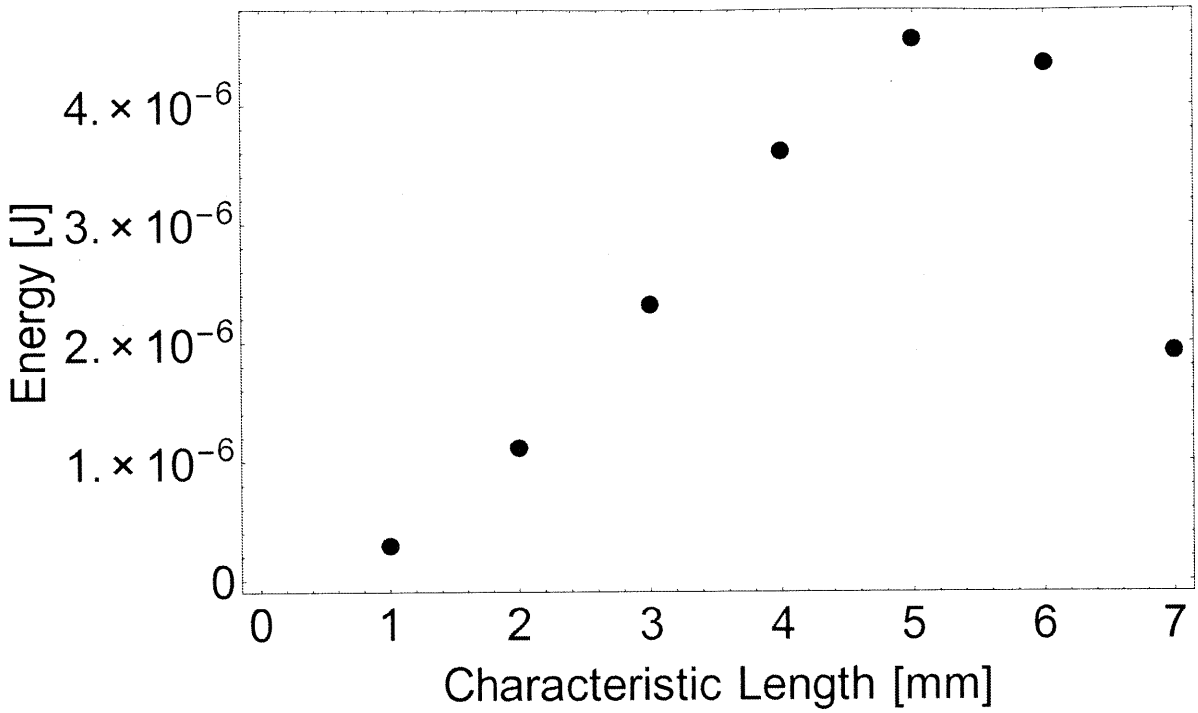

Figure 8. A characteristic length vs. energy plot showing that there is an energy maximum for a bubble on a rod with one unpinned vertex between 4 and 6 mm.

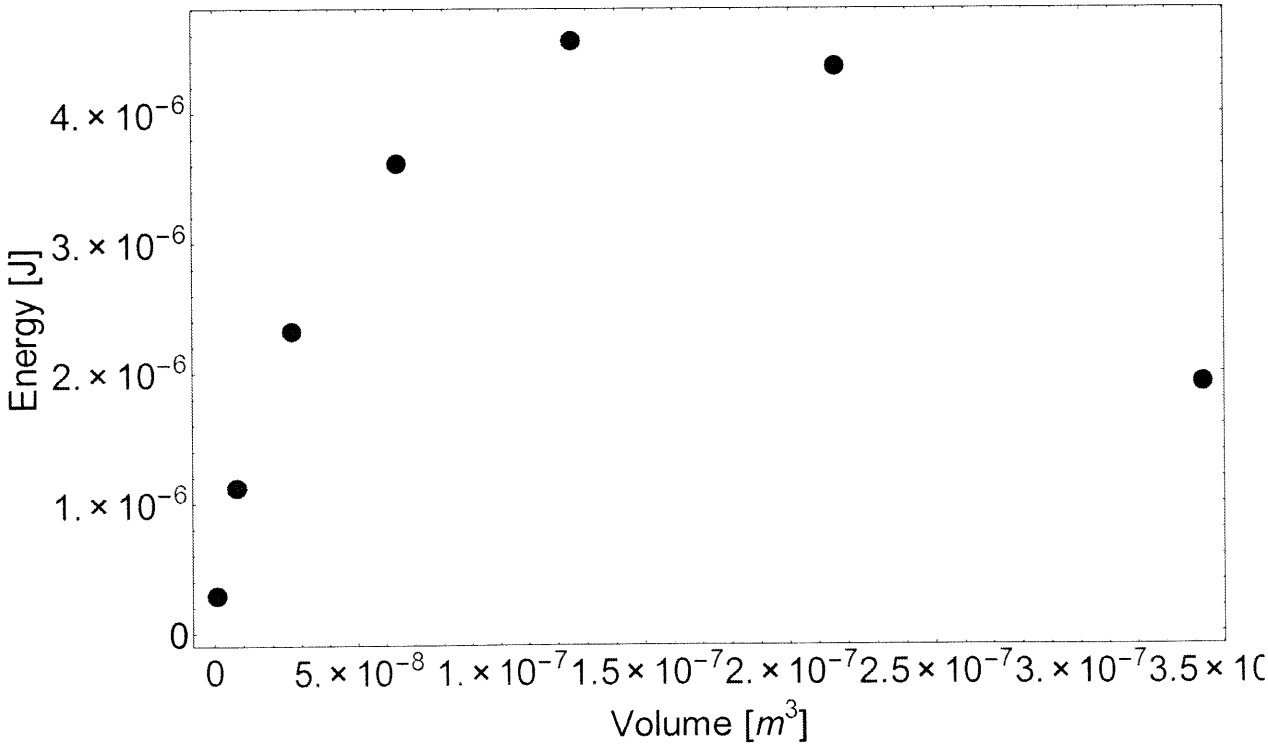

Figure 9. A volume vs. energy plot showing that there is an energy maximum for a bubble on a rod with one unpinned vertex between 4 and 6 mm.

The equilibrium shape of the bubble was obtained after each simulation was performed. Fig. 10 and Fig. 11 present the collection of equilibrium bubbles shapes (side view and bottom-up view) with the characteristic rod length ranging from 1 mm to 7 mm. The equilibrium shape of the bubble with a characteristic rod length of 8 mm is not shown because the shape did not converge to a stable configuration. From the bottom-up view of the bubble on a rod, it appears that one of the vertices of the bubbles is receding away from the corner of the rod.

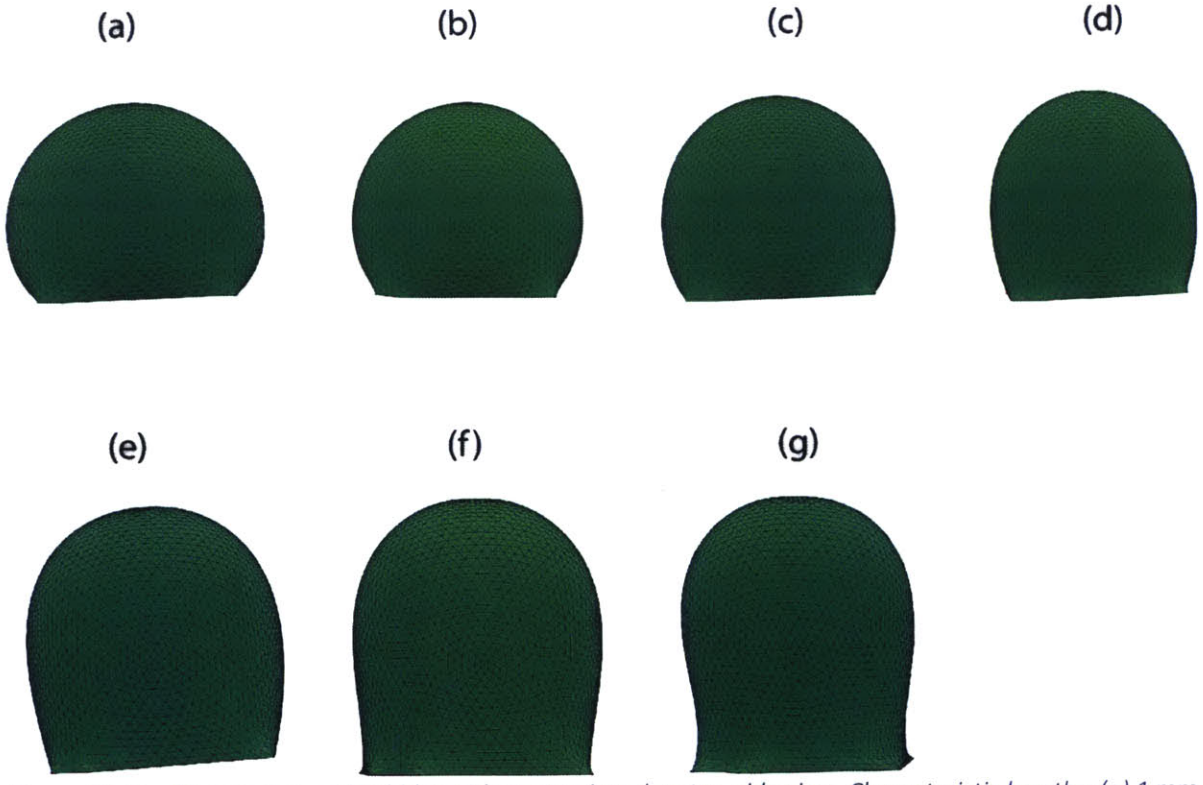

Figure 10. Equilibrium shape of bubbles with one unpinned vertex, side view. Characteristic lengths: (a) 1 mm, (b) 2 mm, (c) 3 mm, (d) 4 mm, (e) 5 mm, (f) 6 mm, (g) 7 mm.

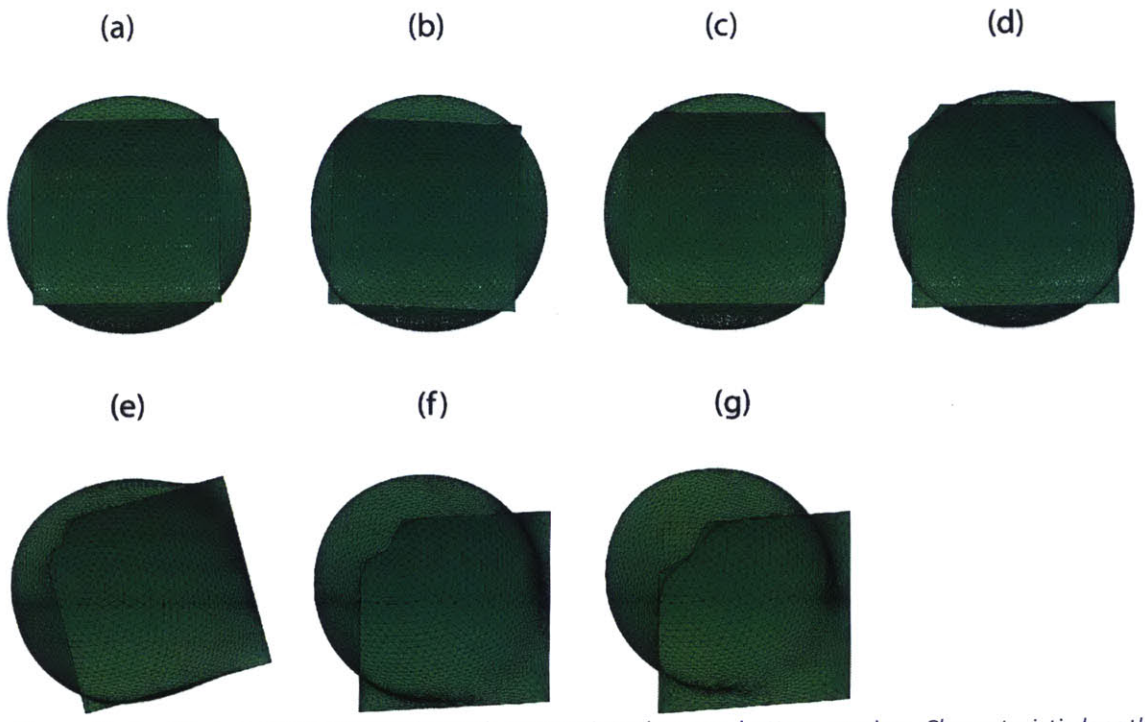

Figure 11. Equilibrium shape of bubbles with one unpinned vertex, bottom-up view. Characteristic lengths: (a) 1 mm, (b) 2 mm, (c) 3 mm, (d) 4 mm, (e) 5 mm, (f) 6 mm, (g) 7 mm.

Detached Bubble

A free spherical bubble (Fig. 12), or one that is completely detached from the surface of the rod, is an optimal system to consider when comparing energies of the equilibrium shapes. Surface Evolver calculates the equilibrium shapes of the surfaces but it is up to the user to determine the possible configurations. There may be stable configurations at a higher energy than the detached bubble. If the detached bubble has the lowest energy of the configurations, than it is the stable shape that the bubble would adopt at a given volume. The other stable configurations would be deemed metastable states.

Figure 12. Schematic of a bubble of radius R completely detached from the rod.

The energy of the system (in which the bubble is completely detached from the rod) can be calculated by determining the surface energy of the detached bubble. The energy of a detached spherical bubble is the following:

$$E = \gamma\, 4\pi r^2 \tag{21}$$

Replacing the radius r in terms of volume of a sphere gives

$$E = \gamma\, 4\pi \left(\frac{3V}{4\pi}\right)^{2/3} \tag{22}$$

Bubble Constrained to Rod Surface with No Pinned Edges

In this study, a bubble is situated on a rod with surface dimensions of 100 nm by 100 nm. The bubble is constrained to lie on the surface of the rod but the edges and vertices of the bubble are not pinned to those of the rod (Appendix, Part B). In all the visuals of the simulations, only the top surface of the rod is depicted. The volume of the bubble was increased in each simulation, giving rise to Fig. 13 (a-h), where the contact angle of the bubble with the surface of the rod was 80 degrees. In all the simulations where the contact angle was 80 degrees, the bubble wet the

surface of the rod completely. As the volume of the bubble increases, the bubble approaches a spherical shape.

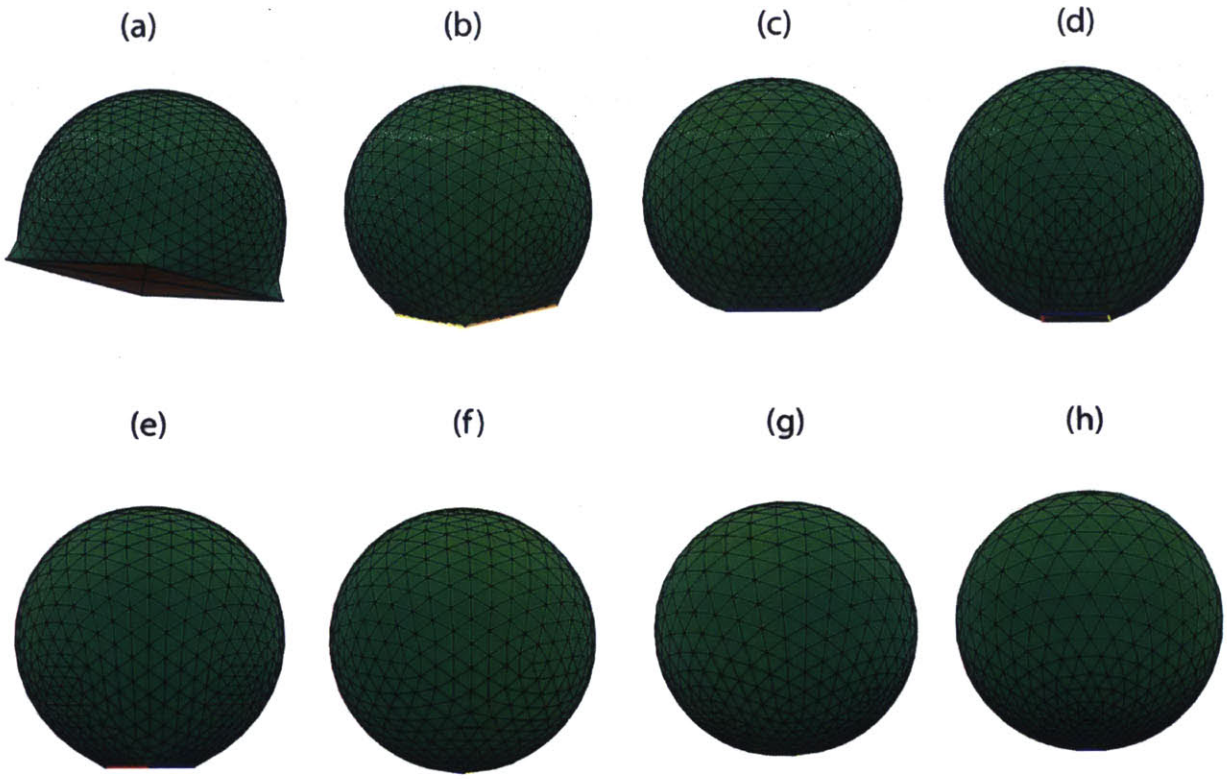

Figure 13. Simulations of a bubble with a contact angle of 80 degrees on a nanorod.

A bubble with a contact angle of 92 degrees was run through simulations to obtain the equilibrium shapes and energy of the system found in Fig. 14 (side view) and 15 (bottom-up view) (Appendix, Part C). In these simulations, the stable equilibrium shape of the bubble did not wet the surface of the rod completely. Similar to the case where the contact angle was 80 degrees, the bubble approached a spherical shape as the volume increased. In Fig. 15, the dimensions of the rod surface stay fixed but the bubble increases in volume.

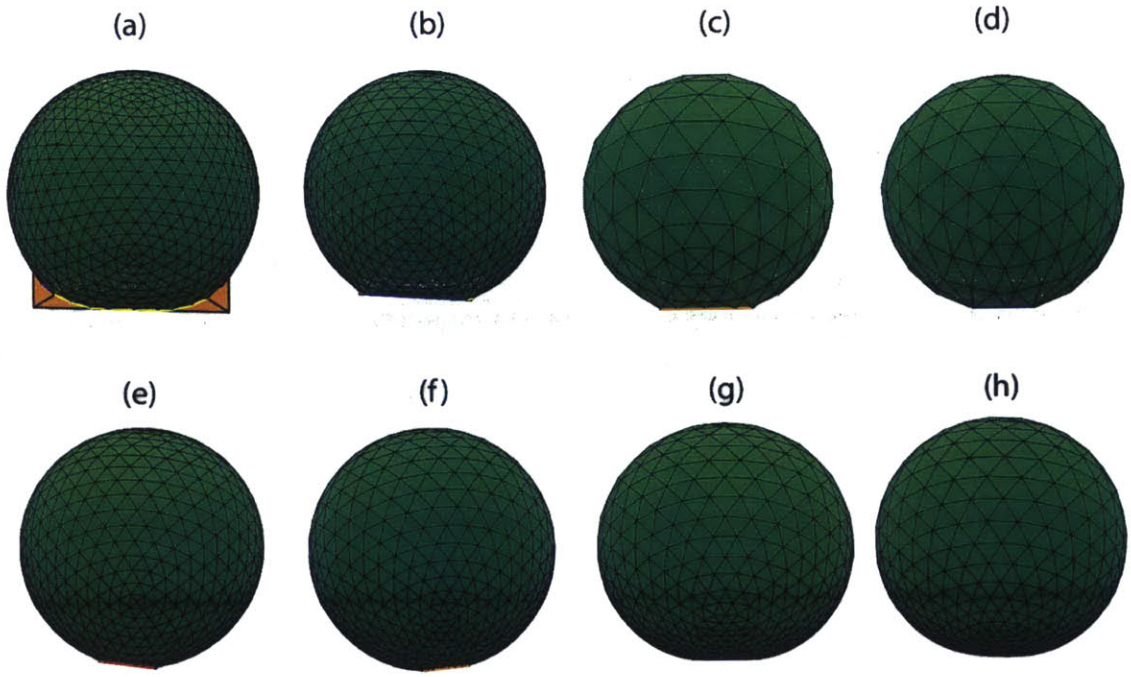

Figure 14. Simulations of a bubble with a contact angle of 92 degrees on a nanorod (side-view).

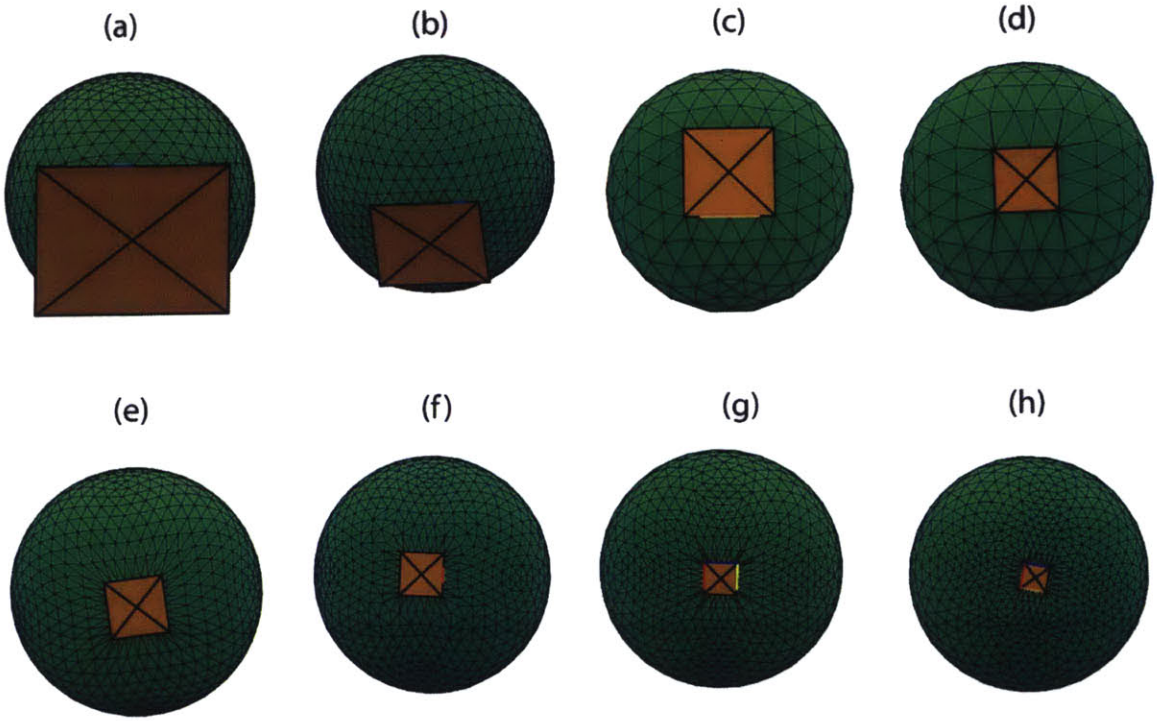

Figure 15. Simulations of a bubble with a contact angle of 92 degrees on a nanorod (bottom-up view). The surface of the nanorod is depicted as a brown square.

The energy of the bubble on a rod (with a contact angle of 80 and 92 degrees) was compared to that of a free spherical bubble (Fig. 16). The energy of this bubble that is attached to the rod approaches the energy of a free spherical bubble with an equivalent volume. The bubble appears to remain attached to the surface of the nanorod but because the initial bubble shape was constrained to lie on the surface of the nanorod, it will never lift off the surface of the nanorod. The important factor is the energy of the total configuration, which approaches the energy of a free sphere as the volume increases.

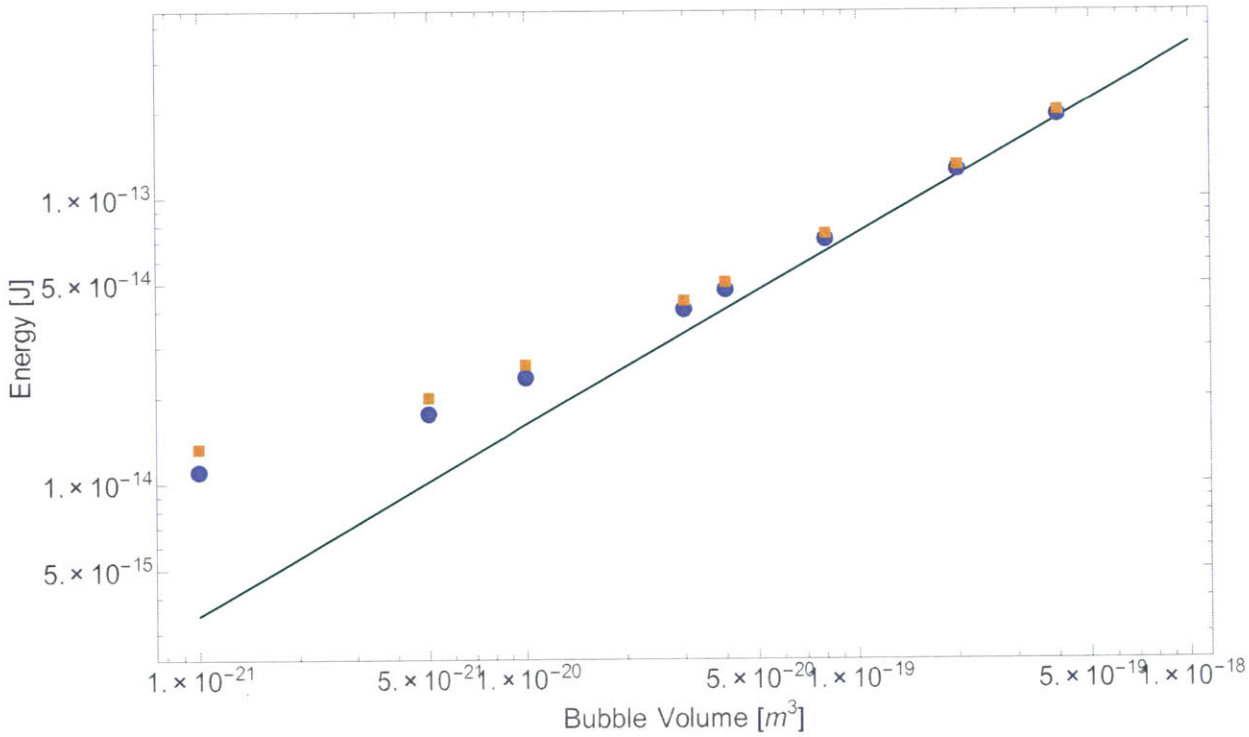

Figure 16. Log-log plot of bubble volume vs. energy. The green line is the energy of a free spherical bubble. The blue circles and orange squares are the energy of the bubble shape with a contact angle of 80 and 92 degrees respectively.

Bubble Constrained to Rod Surface with Multiple Unpinned Edges

A bubble (contact angle of 92 degrees) on a 100 by 100 nm rod was constrained so that one of its edges was unpinned from one edge of the rod. That unpinned edge was free to move on the

surface of the rod but it was not constrained to lie on the edge of the rod (Appendix, Part D). The surface was refined and equilibrated to the shape found in Fig. 17a. A bubble with two of its edges unpinned from the edges of the rod (Appendix, Part E) is depicted in Fig. 17b. The energies of these two configurations were calculated and were numerically equivalent to the energy of a bubble (contact angle 92 degrees) with all edges unpinned.

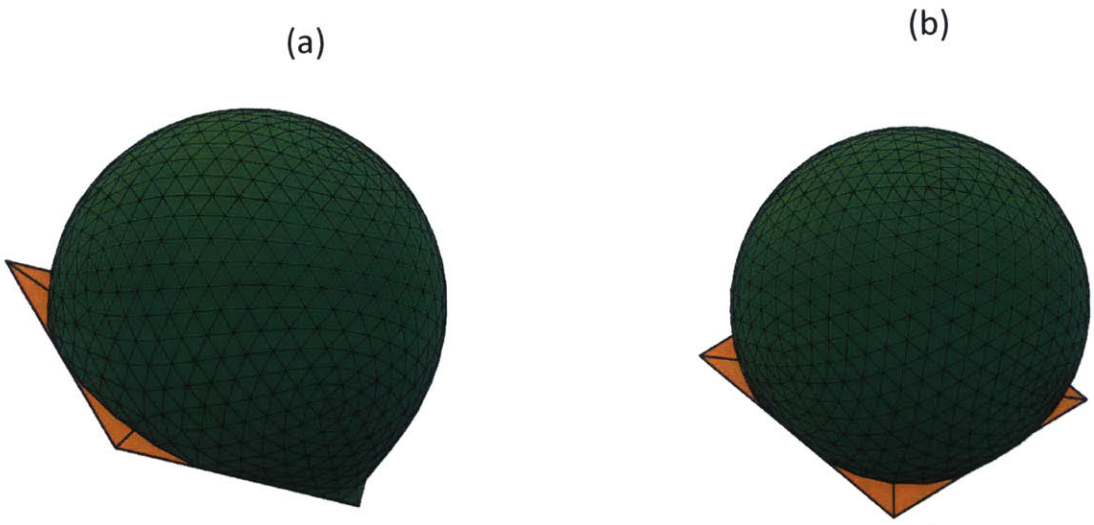

Figure 17. Unpinning one edge (a) and two edges (b) of the bubble from the nanorod.

Conclusions

Successful implementation of Surface Evolver in modeling bubbles on surfaces includes understanding the energy and content integrals, maintaining a robust mesh through refining and eliminating unwanted facets, and computing the lowest energy configurations using a variety of constraints. These techniques form the foundation for modeling a bubble on the surface of a nanorod. A nanorod with a top surface dimension of 100 by 100 nm was the subject of the bulk of this work. The energy of different starting configurations of the bubble and increasing volume of the bubble were compared to that of a free spherical bubble. The energy of the bubble approaches the total surface energy of a free spherical bubble, indicating that a bubble that has nucleated on the surface of a nanorod will approach a shape that has nearly the same energy as a detached spherical bubble. For applications in PEC splitting of water, this result indicates that from an equilibrium and lowest energy perspective, an oxygen bubble could nucleate on the surface of a nanorod, grow in volume, and detach or pinch-off from the nanorod. There are kinetic effects that must be taken into account for a comprehensive model of bubble formation and detachment which was not presently studied. For a model that is able to predict optimal surface morphologies, future work involves computing the stable configurations of a bubble on an increasing variety of surfaces.

References

(1) Sivula, K.; Le Formal, F.; Grätzel, M. *ChemSusChem* **2011**, *4*, 432–449.

(2) Van de Krol, R.; Gratzel, M. *Photoelectrochemical Hydrogen Production*; VIII.; Springer, 2012.

(3) Murphy, A. B. *Int. J. Hydrogen Energy* **2006**.

(4) Brakke, K. A. *Surface Evolver Manual*; 2013.

(5) Berthier, J.; Brakke, K. A. *The Physics of Microdroplets*; Scrivener Publishing LLC., 2012.

(6) Herminghaus, S.; Brinkmann, M.; Seemann, R. *Annu. Rev. Mater. Res.* **2008**, *38*, 101–121.

(7) Batchelor, G. K. *An Introduction to Fluid Dynamics*; Cambridge University Press, 1967.

(8) Checco, A.; Gang, O.; Ocko, B. M. *Phys. Rev. Lett.* **2006**, *96*, 1–4.

(9) Checco, A.; Cai, Y.; Gang, O.; Ocko, B. M. *Ultramicroscopy* **2006**, *106*, 703–708.

(10) Seemann, R.; Jacobs, K.; Blossey, R. *J. Phys.-Condes. Matter* **2001**, *13*, 4915–4923.

(11) Lipowsky, R.; Lenz, P.; Swain, P. S. *Colloids Surfaces A Physicochem. Eng. Asp.* **2000**, *161*, 3–22.

(12) Brennen, C. E. *Cavitation and Bubble Dynamics*; Oxford University Press: Oxford, 1995.

(13) Skripov, V. P. *Metastable Liquids*; Wiley: New York, 1974.

(14) Matsumoto, M.; Tanaka, K. *Fluid Dyn. Res.* **2008**, *40*, 546–553.

(15) G, N.; Tsuruta, T.; Cheng, P. *Int. J. Heat Mass Transf.* **2006**, 4437–4443.

(16) Good, R. J.; Stromberg, R. R. *Surface and Colloid Science*; Plenum Press: New York, 1979.

(17) Drelich, J.; Miller, J. D.; Good, R. J. *J. Colloid Interface Sci.* **1996**, *179*, 37–50.

(18) Vos, V. S. S. Deformations of a bubble, Universiteit Leiden, 2012.

Appendix

The following are the datafiles for the Surface Evolver simulations.

Part A

Bubble on Rod- one unpinned vertex. Example with characteristic rod length as 4000 microns.

```
//Bubble on Rod (4000 micron side lengths)
//One of the vertices is unpinned from the edge constraints
// ____________________________________________________________

gravity_constant -9.8
parameter TENS   = 0.072   //surface tension of water in contact with air

parameter AA = 4000e-6      //rod is 4000 microns on each side
parameter BB = AA*AA*AA    //volume of bubble is
parameter angle = 90

#define TENSION (-cos(angle*pi/180))

constraint 10
formula: z = 0
energy:
e1: 0
e2: TENSION*x
e3: 0


constraint 1
formula: x = 0

constraint 2
formula: x = AA

constraint 3
formula: y = AA

constraint 4
formula: y = 0

//scale_limit 1/TENS
```

vertices

// drop contacting surface
1 0.0 0.0 0.0 constraint 10 //unpinned from edges
2 AA 0.0 0.0 constraint 10 2 4
3 AA AA 0.0 constraint 10 2 3
4 0.0 AA 0.0 constraint 10 1 3
//top of initial drop
5 0.0 0.0 AA
6 AA 0.0 AA
7 AA AA AA
8 0.0 AA AA

edges
//edges contacting surface
1 1 2 constraint 4 10
2 2 3 constraint 2 10
3 3 4 constraint 3 10
4 4 1 constraint 1 10
//top edges of drop
5 5 6
6 6 7
7 7 8
8 8 5
//side edges of drop
9 1 5
10 2 6
11 3 7
12 4 8

faces
1 1 10 -5 -9 tension TENS color green
2 2 11 -6 -10 tension TENS color green
3 3 12 -7 -11 tension TENS color green
4 4 9 -8 -12 tension TENS color green
5 5 6 7 8 tension TENS color green

bodies
1 1 2 3 4 5 volume BB density 1000

Part B

Bubble on Rod- All bubble edges **not** constrained to rod edges, rod is 100 nm on each side; contact angle is 80 degrees

```
// _____________________________________________________________________
//Unpinned all vertices and edges contacting top surface of rod

gravity_constant -9.8
parameter TENS   = 0.072   //surface tension of water in contact with air

parameter AA = 100e-9      //rod is 100nm on each side
parameter BB = AA*AA*AA    //volume of bubble is
parameter angle = 80

#define TENSION (-cos(angle*pi/180))

constraint 10
formula: z = 0
energy:
e1: 0
e2: TENSION*x
e3: 0

constraint 5 nonnegative
formula: y

constraint 6 nonpositive
formula: y-AA

constraint 7 nonnegative
formula: x

constraint 8 nonpositive
formula: x-AA


//scale_limit 1/TENS


vertices


// drop contacting surface
1 0.0 0.0 0.0 constraint 10 5 6 7 8
2 AA 0.0 0.0 constraint 10 5 6 7 8
3 AA AA 0.0 constraint 10 5 6 7 8
4 0.0 AA 0.0 constraint 10 5 6 7 8
//top of initial drop
5 0.0 0.0 AA
6 AA 0.0 AA
```

```
7 AA AA AA
8 0.0 AA AA

//substrate
21 0.0 0.0 0.0  fixed
22 AA 0.0 0.0  fixed
23 AA AA 0.0  fixed
24 0.0 AA 0.0 fixed


edges
//edges contacting surface
1 1 2 constraint 10 5 6 7 8  color red
2 2 3 constraint 10 5 6 7 8  color blue
3 3 4 constraint 10 5 6 7 8  color yellow
4 4 1 constraint 10 5 6 7 8  color brown
//top edges of drop
5 5 6
6 6 7
7 7 8
8 8 5
//side edges of drop
9  1 5
10 2 6
11 3 7
12 4 8

//sustrate edges
21 21 22 fixed no_refine
22 22 23 fixed no_refine
23 23 24 fixed no_refine
24 24 21 fixed no_refine

faces
1   1 10 -5  -9 tension TENS color green
2   2 11 -6 -10 tension TENS color green
3   3 12 -7 -11 tension TENS color green
4   4  9 -8 -12 tension TENS color green
5   5  6  7   8 tension TENS color green
6   21  22  23   24 fixed no_refine color brown


bodies
1 1 2 3 4 5 volume BB density 1000
```

Part C

Bubble on Rod- All bubble edges **not** constrained to rod edges, rod is 100 nm on each side; contact angle is 92 degrees

```
// _____________________________________________________________________
//Unpinned all vertices and edges contacting top surface of rod

gravity_constant -9.8
parameter TENS   = 0.072   //surface tension of water in contact with air

parameter AA = 100e-9      //rod is 100nm on each side
parameter BB = AA*AA*AA    //volume of bubble is
parameter angle = 80

#define TENSION (-cos(angle*pi/180))

constraint 10
formula: z = 0
energy:
e1: 0
e2: TENSION*x
e3: 0

constraint 5 nonnegative
formula: y

constraint 6 nonpositive
formula: y-AA

constraint 7 nonnegative
formula: x

constraint 8 nonpositive
formula: x-AA


//scale_limit 1/TENS


vertices


// drop contacting surface
1 0.0 0.0 0.0 constraint 10 5 6 7 8
2 AA 0.0 0.0 constraint 10 5 6 7 8
3 AA AA 0.0 constraint 10 5 6 7 8
4 0.0 AA 0.0 constraint 10 5 6 7 8
//top of initial drop
5 0.0 0.0 AA
6 AA 0.0 AA
```

```
7 AA AA AA
8 0.0 AA AA

//substrate
21 0.0 0.0 0.0  fixed
22 AA 0.0 0.0  fixed
23 AA AA 0.0  fixed
24 0.0 AA 0.0 fixed


edges
//edges contacting surface
1 1 2 constraint 10 5 6 7 8  color red
2 2 3 constraint 10 5 6 7 8  color blue
3 3 4 constraint 10 5 6 7 8  color yellow
4 4 1 constraint 10 5 6 7 8  color brown
//top edges of drop
5 5 6
6 6 7
7 7 8
8 8 5
//side edges of drop
9  1 5
10 2 6
11 3 7
12 4 8

//sustrate edges
21 21 22 fixed no_refine
22 22 23 fixed no_refine
23 23 24 fixed no_refine
24 24 21 fixed no_refine

faces
1   1 10 -5  -9 tension TENS color green
2   2 11 -6 -10 tension TENS color green
3   3 12 -7 -11 tension TENS color green
4   4  9 -8 -12 tension TENS color green
5   5  6  7   8 tension TENS color green
6   21  22  23   24 fixed no_refine color brown


bodies
1 1 2 3 4 5 volume BB density 1000
```

Part D

One edge unpinned

```
// ____________________________________________________________________

gravity_constant -9.8 //buoyancy force
parameter TENS   = 0.072   //surface tension of water in contact with air

parameter AA = 100e-9      //rod is 100 nm on each side
parameter BB = AA*AA*AA   //volume of bubble is


constraint 1
formula: x = 0

constraint 2
formula: x = AA

constraint 3
formula: y = AA

constraint 4
formula: y = 0

constraint 5 nonnegative
formula: y

parameter angle = 92

#define TENSION (-cos(angle*pi/180))

constraint 10
formula: z = 0
energy:
e1: 0
e2: TENSION*x
e3: 0


vertices


// drop contacting surface
1 0.0 0 0.0 constraint 10 1 5
2 AA 0 0.0 constraint 10 2 5
```

```
3 AA AA 0.0 constraint 10 2 3
4 0.0 AA 0.0 constraint 10 1 3
//top of initial drop
5 0.0 0 AA
6 AA 0 AA
7 AA AA AA
8 0.0 AA AA

//substrate
21 0.0 0.0 0.0  fixed
22 AA 0.0 0.0  fixed
23 AA AA 0.0  fixed
24 0.0 AA 0.0 fixed
edges
//edges contacting surface
1 1 2 constraint 10 5
2 2 3 constraint 2 10
3 3 4 constraint 3 10
4 4 1 constraint 1 10
//top edges of drop
5 5 6
6 6 7
7 7 8
8 8 5
//side edges of drop
9  1 5
10 2 6
11 3 7
12 4 8

//sustrate edges
21 21 22 fixed no_refine
22 22 23 fixed no_refine
23 23 24 fixed no_refine
24 24 21 fixed no_refine

faces
1   1 10 -5  -9 tension TENS color green
2   2 11 -6 -10 tension TENS color green
3   3 12 -7 -11 tension TENS color green
4   4  9 -8 -12 tension TENS color green
5   5  6  7   8 tension TENS color green
6   21  22  23   24 fixed no_refine color brown

bodies
1 1 2 3 4 5 volume BB density 1000
```

Part E

Two edges upinned

```
// ____________________________________________________________________________
gravity_constant -9.8 //buoyancy force
parameter TENS   = 0.072   //surface tension of water in contact with air

parameter AA = 100e-9      //rod is 100 nm on each side
parameter BB = AA*AA*AA   //volume of bubble is

constraint 1
formula: x = 0

constraint 2
formula: x = AA

constraint 3
formula: y = AA

constraint 4
formula: y = 0

constraint 5 nonnegative
formula: y

constraint 6 nonpositive
formula: y-AA

constraint 8 nonpositive
formula: x-AA

parameter angle = 92

#define TENSION (-cos(angle*pi/180))

constraint 10
formula: z = 0
energy:
e1: 0
e2: TENSION*x
e3: 0

vertices
// drop contacting surface
1 0.0 0 0.0 constraint 10 1 5
2 AA 0 0.0 constraint 10 5 8
```

```
3 AA AA 0.0 constraint 10 8 6
4 0.0 AA 0.0 constraint 10 1 3
//top of initial drop
5 0.0 0 AA
6 AA 0 AA
7 AA AA AA
8 0.0 AA AA

//substrate
21 0.0 0.0 0.0  fixed
22 AA 0.0 0.0  fixed
23 AA AA 0.0  fixed
24 0.0 AA 0.0 fixed

edges
//edges contacting surface
1 1 2 constraint 10 5
2 2 3 constraint 10 8
3 3 4 constraint 10 6
4 4 1 constraint 1 10
//top edges of drop
5 5 6
6 6 7
7 7 8
8 8 5
//side edges of drop
9  1 5
10 2 6
11 3 7
12 4 8
//sustrate edges
21 21 22 fixed no_refine
22 22 23 fixed no_refine
23 23 24 fixed no_refine
24 24 21 fixed no_refine

faces
1   1 10 -5  -9 tension TENS color green
2   2 11 -6 -10 tension TENS color green
3   3 12 -7 -11 tension TENS color green
4   4  9 -8 -12 tension TENS color green
5   5  6  7   8 tension TENS color green
6   21  22  23   24 fixed no_refine color brown

bodies
1 1 2 3 4 5 volume BB density 1000
```